inorganics

MDPI

Article

Synthesis and Functionalization of a 1,2-Bis(trimethylsilyl)-1,2-disilacyclohexene That Can Serve as a Unit of *cis*-1,2-Dialkyldisilene

Naohiko Akasaka, Kaho Tanaka, Shintaro Ishida and Takeaki Iwamoto *

Department of Chemistry, Graduate School of Science, Tohoku University, Aoba-ku, Sendai 980-8578, Japan; nao.akasaka1216@gmail.com (N.A.); kaho.tanaka.q2@dc.tohoku.ac.jp (K.T.); sishida@m.tohoku.ac.jp (S.I.)
* Correspondence: iwamoto@m.tohoku.ac.jp; Tel.: +81-22-795-6558

Received: 5 January 2018; Accepted: 17 January 2018; Published: 24 January 2018

Abstract: π-Electron compounds that include multiple bonds between silicon atoms have received much attention as novel functional silicon compounds. In the present paper, 1,2-bis(trimethylsilyl)-1,2-disilacyclohexene **1** was successfully synthesized as thermally stable yellow crystals. Disilene **1** was easily converted to the corresponding potassium disilenide **4**, which furnished novel functionalized disilenes after the subsequent addition of an electrophile. Interestingly, two trimethylsilyl groups in **1** can be stepwise converted to anthryl groups. The novel disilenes derived from **1** were characterized by a combination of nuclear magnetic resonance (NMR) spectroscopy, mass spectrometry (MS), elemental analyses, and X-ray single crystal diffraction analysis. The present study demonstrates that disilene **1** can serve as a unit of *cis*-1,2-dialkyldisilene.

Keywords: disilene; functionalization; π-electron systems

1. Introduction

Stable silicon compounds that include double bonds between silicon atoms (disilenes, $R_2Si{=}SiR_2$) have received much attention over the last three decades [1–3]. Because such silicon π-electron systems have an intrinsically higher π-orbital level and a narrower HOMO (highest occupied molecular orbital)–LUMO (lowest unoccupied molecular orbital) gap compared to those of the corresponding organic π-electron systems, extended π-electron systems that include the Si=Si double bond(s) should be anticipated to be unprecedented functional π-electron materials. In this context, the reactions of disilenide (a disilicon analogue of vinyl anion $[R_2Si{=}SiR]^-$) with electrophiles is one of the promising routes to introduce a functional group into the silicon π-electron systems [4–9]. Disilenides have been synthesized by reductive dehalogenation of the corresponding trihalodisilane [10] or reductive cleavage of R–Si(sp^2) bond on the Si=Si double bond in a stable disilene [11–15].

Very recently, we found a novel route to a disilenide from a stable disilene under milder conditions [16]. In this route, the disilenide was generated from the reaction of a trimethylsilyl-substituted disilene and potassium *t*-butoxide [17] via selective cleavage of the Si(sp^2)–Si(sp^3) bond on the Si=Si double bond. In this reaction, neither an undesired reduction of the Si=Si double bond nor addition of *t*-BuOK across the Si=Si double bond occurred. During the course of our study, we designed a novel cyclic disilene, 1,2-bis(trimethylsilyl)-substituted 1,2-disilacyclohexene **1**. Compound **1** has two trimethylsilyl groups that can be converted stepwise to the corresponding potassium derivatives after treatment of *t*-BuOK, as well as alkyl groups that cause at least perturbation to the electronic structure of the Si=Si double bond and should be suitable for the investigation of interactions between the Si=Si double bond and the functional group. Herein, we report successful synthesis, molecular structure and functionalization of **1** and its derivatives. Although **1** has six trimethylsilyl groups on the six-membered ring, one trimethylsilyl group on the Si=Si double

bond is selectively eliminated to provide the corresponding disilenide after treatment with *t*-BuOK. Noticeably, two trimethylsilyl groups in **1** were converted stepwise to anthryl groups to furnish the corresponding 1,2-dianthryldisilene in good yield.

2. Results and Discussion

2.1. Synthesis and Molecular Structure of Disilacyclohexene **1**

1,2-Bis(trimethylsilyl)-1,2-disilacyclohexene **1** was synthesized as shown in Scheme 1 similar to that of 1,2-diphenyl-3,3,6,6-tetrakis(trimethylsilyl)-1,2-disilacyclohexene **A** [18] (Figure 1). The reaction of Me_3SiSiH_2Cl, which was generated by the reaction of Me_3SiSiH_2Ph with triflic acid followed by addition of NEt_3·HCl salt, with 1,4-dilithio-1,1,4,4-tetrakis(trimethylsilyl)butane, which was also generated from 1,1-bis(trimethylsilyl)ethene and lithium in tetrahydrofuran (THF), afforded 1,4-bis(2,2,2-trimethyldisilanyl)butane **2** in 89% yield. Bromination of **2** with Br_2 provided tetrabromo derivative **3** in 70% yield. Finally, treatment of **3** with potassium graphite (KC_8) in THF furnish **1** in 99% yield as yellow crystals. The structure of **1** was determined by a combination of multinuclear nuclear magnetic resonance (NMR) spectroscopy, mass spectrometry (MS) and X-ray diffraction (XRD) analysis (Figure 2, Table 1 (vide infra)). The six-membered ring of **1** adopts a half-chair conformation similar to the corresponding 1,2-diphenyl derivative **A**. The Si1–Si2 bond length in **1** (2.1762(5) Å) is slightly longer than that in **A** (2.1595(5) Å). The geometry around the Si=Si double bond of **1** is trans-bent and twisted; bent angles β of **1** (Si1: 12.9°; Si2: 6.5° (Si2)) are smaller than those of **A** (Si1: 13.7°; Si2: 19.2° (Si2)), while the twist angle τ of **1** (17.7°) is larger than that of **A** (4.8°). These substantial differences in the geometry around the Si=Si bond would be due to a combination of the electronic effects of silyl substituents that favor a planar geometry [19–21] and the steric effects of the silyl substituents, as the potential energy surface of the bending of the Si=Si double bond has been predicted to be shallow [20,22]. In ^{1}H, ^{13}C and ^{29}Si NMR spectra, three singlet signals of trimethylsilyl groups (one is on the unsaturated silicon atom and the other two are on the alkyl substituent), which indicates that the ring inversion occurs slowly on the NMR time scale in solution. The ^{29}Si resonance of unsaturated silicon nuclei of **3** (131.4 ppm) are slightly downfield-shifted compared to that of **A** (100.9 ppm), which should be due to the substituent effects of silyl group on the Si=Si double bond [23]. In the UV–Vis absorption spectrum of **1** in hexane, a distinct absorption band assignable to a π(Si=Si)→π*(Si=Si) transition (see, Figure S46) appeared at 420 nm (ε 1.57 × 10^4), which is slightly hypsochromically shifted compared to that of **A** (427 nm (ε 8400) in hexane).

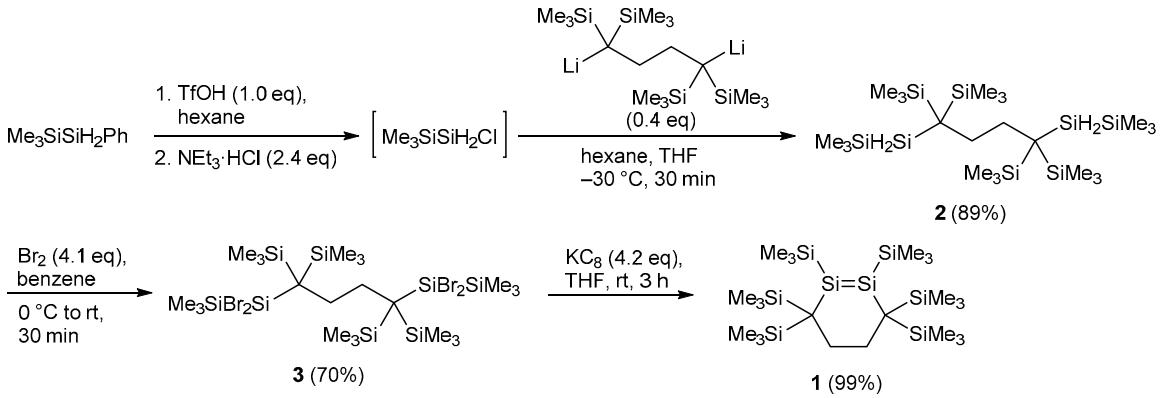

Scheme 1. Synthesis of disilene **1**.

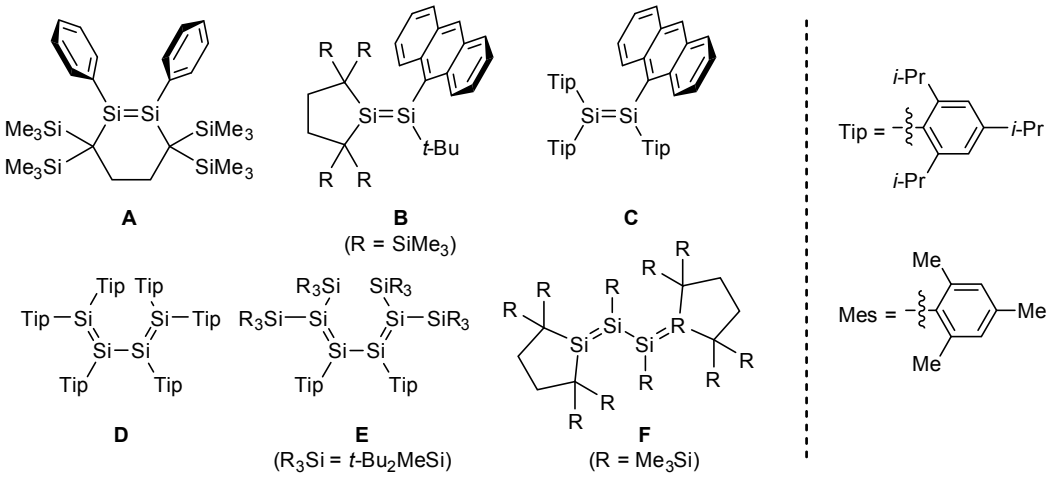

Figure 1. Related disilenes **A** [18], **B** [10], and **C** [24], as well as tetrasila-1,3-dienes **D** [25], **E** [12], and **F** [26].

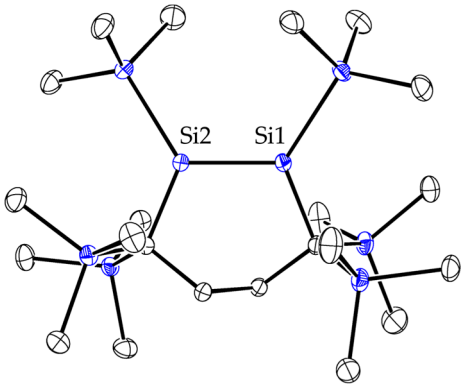

Figure 2. ORTEP (Oak Ridge Thermal Ellipsoid Plot) drawing of **1** with thermal ellipsoids set at 50% probability and hydrogen atoms omitted for clarity.

2.2. *Conversion of* **1** *to Disilenide* **4** *and Functionalized Disilenes*

Disilene **1** can be effectively converted to the corresponding disilenide through a selective cleavage of the Si(sp^2)–Si(sp^3) bond (Scheme 2) [16]. When **1** was treated with one equivalent of *t*-BuOK in THF, the color of solution gradually turned from yellow to orange. The formation of potassium disilenide **4** as a sole product in the resulting reaction mixture was confirmed by a combination of the multinuclear NMR spectra in C_6D_6 and the results of the reaction with electrophiles (vide infra). In this reaction, 1,2-addition of *t*-BuOK across the Si=Si double bond of **1** as well as elimination of a trimethylsilyl group on the carbon atom in the disilacyclohexene ring was not observed at all. The ^{1}H, ^{13}C, and ^{29}Si NMR spectra of **4**(thf) in C_6D_6 exhibits the presence of five trimethylsilyl groups. The ^{29}Si NMR spectra exhibited two signals due to the unsaturated silicon nuclei at 146.9 ppm (=*Si*SiMe$_3$) and 219.3 ppm (=*Si*$^-$). Similar large differences between the chemical shifts of the unsaturated silicon nuclei have been found in those of structurally related disilenides (Me$_3$Si)TipSi=SiTip[K(thf)$_n$] (101.4 (=*Si*(SiMe$_3$)Tip), 186.6 (=*Si*$^-$) in THF-d_8; Tip = 2,4,6-triisopropylphenyl) [16] and reported disilenides [27].

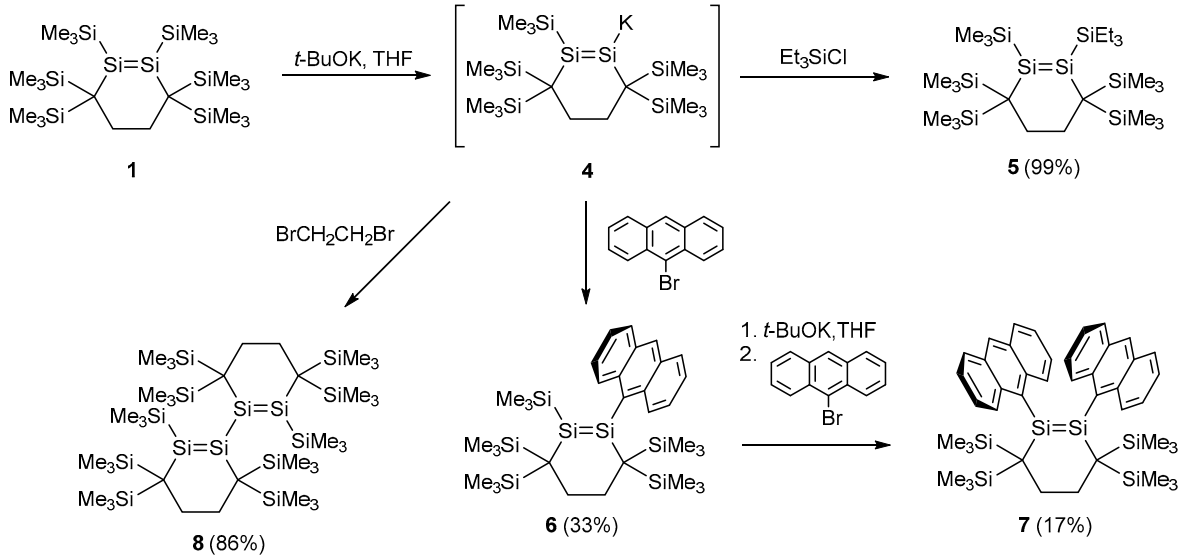

Scheme 2. Synthesis of functionalized disilenes through desilylation of **1**.

After removal of the volatiles, recrystallization from toluene provided suitable single crystals of (**4**(toluene))$_2$. In the single crystals, disilenide **4** forms a dimer with a crystallographic inversion center (Figure 3a). Interestingly, the potassium cations are coordinated by one anionic silicon atom in an η^1-fashion, one toluene molecule in an η^6-fashion, and the Si=Si double bond in the other disilenide moiety in an η^2-fashion. The distance of Si1–K1 is 3.4655(5) Å, which falls in typical range of Si1–K1 distance in the reported potassium disilenides (3.33–3.52 Å) [10,13,28], while the Si1···K1′ and Si2···K1′ distances are 3.5066(5) and 3.7645(5) Å. Although the dimeric structure of metal disilenides in the solid state have been reported [10,28,29], to the best of our knowledge, such η^2-coordination of the Si=Si double bond in a disilenide to the metal cation in the solid state is unprecedented. The Si=Si distance in (**4**(toluene))$_2$ (2.2035(5) Å) is substantially elongated compared that of neutral disilene **1** (2.1762(5) Å) and the geometry around the Si=Si double bond is slightly *cis*-bent (bent angle β: 3.7° (*Si1*–K1), 1.5° (*Si2*–SiMe$_3$); twist angle τ: 1.5°), which may result from the η^2-coordination of the Si=Si double bond to the K cation.

Treatment of **4**, which was generated from **1** and *t*-BuOK in THF, with an electrophile provide various functionalized disilenes (Scheme 2). For instance, reaction of **4** with triethylchlorosilane gave Et$_3$Si-substituted disilene **5** as yellow crystals in 99% yield. The reaction of **4** with one equivalent of 9-bromoanthracene furnished the corresponding anthryldisilene **6** (33% yield). In a similar manner, (10-bromo-9-anthryl)disilene **6^{Br}** was obtained as a major product from the reaction of **4** and one equivalent of 9,10-dibromoanthracene, although it was not obtained in a pure form due to the inseparable byproducts such as anthracene and 9-bromoanthracene. Although the reactions of **4** with less bulky bromoarenes such as bromobenzene or bromomesitylene (2,4,6-trimethylbromobenzene) afforded a mixture which may contain the desired phenyl or mesityl-substituted disilenes, isolation of these disilenes was unsuccessful probably due to the instability of the resulting less bulky aryldisilenes under these reaction conditions. Noticeably, disilene **6** underwent a further desilylation reaction followed by addition of 9-bromoanthracene to furnish 1,2-dianthryldisilene **7** as black purple crystals in 17% yield. The reaction of **4** with 0.5 equivalent of 1,2-dibromoethane afforded the corresponding tetrasiladiene **8** in 86% yield as red-orange crystals similar to the reaction of Tip$_2$Si=SiTipLi and mesityl bromide leading to the corresponding hexaryltetrasila-1,3-diene **D** (Figure 1) [25].

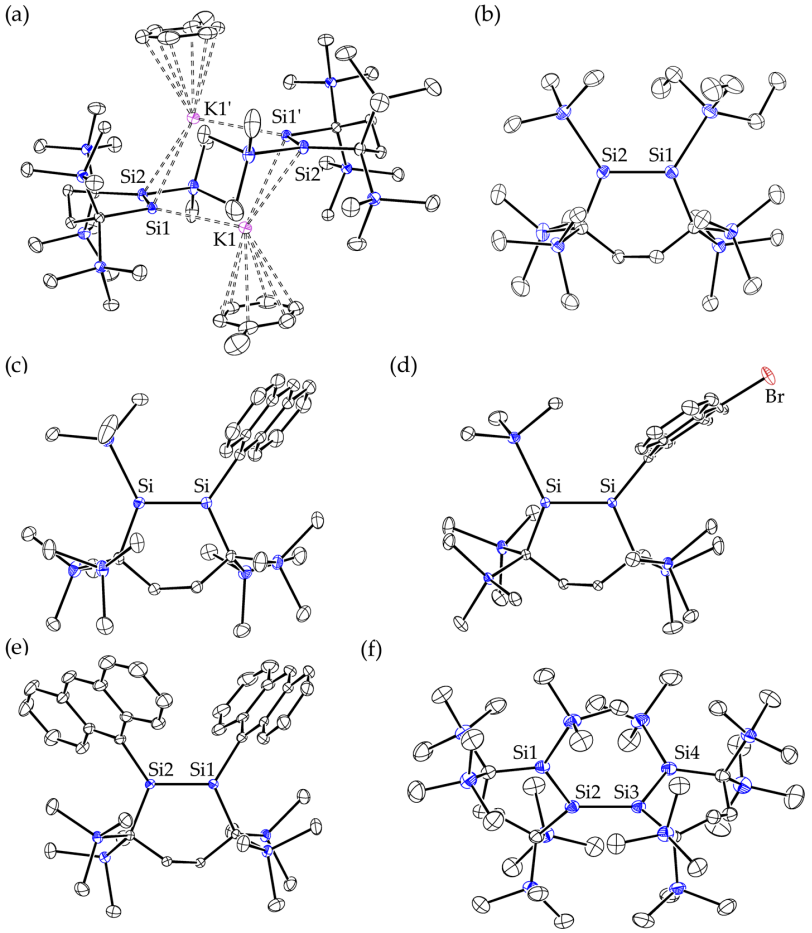

Figure 3. ORTEP drawings of (**a**) (**4**(toluene))$_2$, (**b**) **5**, (**c**) **6**, (**d**) **6**$^{\mathbf{Br}}$, (**e**) **7**, and (**f**) **8** with thermal ellipsoids set at 50% probability and hydrogen atoms omitted for clarity.

Table 1. Selected structural parameters and spectral data of disilenes.

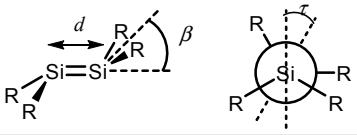

Cpd	*d*/Å	Angle Sum at Si/°	*β*/°	*τ*/°	*δ*(^{29}Si) [1]	λ_{max}/nm (*ε*) [2]
1	2.1762(5)	358.52(3) (*Si1*–$SiMe_3$), 359.61(3) (*Si2*–$SiMe_3$)	12.9 (*Si1*–$SiMe_3$), 6.5 (*Si2*–$SiMe_3$)	17.7	131.4 (=*Si*–$SiMe_3$)	420 (1.57 × 10^4), 343 (4.63 × 10^3)
4	2.2035(5)	358.04(3) (=*Si*···K), 359.94(3) (=*Si*–$SiMe_3$)	3.7 (=*Si*···K) [3], 1.5 (=*Si*–$SiMe_3$) [3]	2.5	146.9 (=*Si*–$SiMe_3$) 219.3 (=Si^-)	–
5	2.1860(19)	358.8(1) (=*Si*–$SiEt_3$), 358.6(1) (=*Si*–$SiMe_3$)	11.2 (=*Si*–$SiEt_3$), 12.1 (=*Si*–$SiMe_3$)	17.6	123.5 (=*Si*–$SiEt_3$), 134.2 (=*Si*–$SiMe_3$)	–
6	2.1598(6)	360.00(5) (=*Si*–Ant), 355.98(3) (=*Si*–$SiMe_3$)	0.1 (=*Si*–Ant), 22.5 (=*Si*–$SiMe_3$)	0.1	130.3 (=*Si*–Ant), 74.9 (=*Si*–$SiMe_3$)	535 (9.25 × 10^2), 399 (2.64 × 10^4)
6$^{\mathbf{Br}}$	2.1711(7)	359.76(6) (=*Si*–Ant^{Br}), 356.04(5) (=*Si*–$SiMe_3$)	4.7 (=*Si*–Ant^{Br}), 22.4 (=*Si*–$SiMe_3$)	8.5	75.1 (=*Si*–$SiMe_3$), 129.1 (=*Si*–Ant^{Br})	[578 (9.67 × 10^2), 410 (3.08 × 104)] [5]
7	2.1525(7)	357.10(6) (*Si1*–Ant), 355.71(6) (*Si2*–Ant)	17.4 (=*Si1*–Ant), 21.0 (=*Si2*–Ant)	3.3	88.2 (=*Si*–Ant)	543 (1.68 × 10^3) 399 (1.85 × 10^4)
8 [4]	2.1850(4) (*Si1*=*Si2*) 2.1915(5) (*Si3*=*Si4*)	359.99(4) (*Si1*), 359.99(3) (*Si2*) 359.98(3) (*Si3*) 359.94(4) (*Si4*)	0.3 (*Si1*) 1.2 (*Si2*) 1.0 (*Si3*) 2.4 (*Si4*)	0.7 (*Si1*=*Si2*) 1.8 (*Si3*=*Si4*)	106.4 (*Si*=$SiSiMe_3$), 143.0 (Si=*Si*$SiMe_3$)	~500 (sh, 3.57 × 10^3), 437 (3.42 × 10^4)

[1] Measured in benzene-d_6. [2] Measured in hexane. [3] *cis*-bent. [4] Dihedral angle Si1–Si2–Si3–Si4 = −88.36(2)°. [5] The sample contains **6** (~10%).

2.3. Molecular Structures of Disilenes **5**–**8**

Similar to **1**, the Si=Si double bond in triethylsilyl-substituted disilene **5** adopts a *trans*-bent and twist geometry (Figure 3b, Table 1): the Si=Si double bond distance (2.1860(19) Å) is slightly longer than that in **1** (2.1762(5) Å) possibly due to the increased steric bulkiness of the silyl group. The ^{29}Si chemical shifts of double bonded Si nuclei in **5** (123.5 (*Si*–$SiEt_3$) and 134.2 ppm (*Si*–$SiMe_3$)) are close to that of **1** (131.4 ppm).

Monoanthryldisilene **6** has a slightly shorter Si=Si double bond distance (2.1598(6) Å) compared to that of **1** (Figure 3c). The geometry around the Si atom bonded to the anthryl group is almost planar (the angle sum: 360.00(5)°), while that bonded to the $SiMe_3$ group is significantly pyramidalized (355.98 (3)°). Such larger pyramidalization at the silyl-substituted silicon center compared to that at the phenyl-substituted center have been predicted theoretically in an unsymmetrical substituted disilene $Ph_2Si{=}Si(SiH_3)_2$ [30]. The disilene π (π*Si*) and aromatic π (π*C*) systems are almost perpendicular to each other (dihedral angle δ: 76.0°). A similar structural feature was found in 10-bromoanthryl-substituted disilene $\mathbf{6^{Br}}$ (the angle sum: 359.76(6)° (*Si*–Ant^{Br}), 356.04(5)° (*Si*–$SiMe_3$); dihedral angle δ: 81.9°) except for the longer Si=Si double bond distance (2.1711(7) Å) (Figure 3d). Although the structural characteristics of **6** and $\mathbf{6^{Br}}$ were essentially consistent with the optimized structures of **6** and $\mathbf{6^{Br}}$ ($\mathbf{6_{opt}}$ and $\mathbf{6^{Br}_{opt}}$) at the B3PW91-D3/6-31G(d) level of theory (Table S6), the Si=Si distance of $\mathbf{6^{Br}}$ (2.1711(7) Å) observed in the single crystals is considerably longer than that of the calculated value of $\mathbf{6^{Br}_{opt}}$ (2.1574 Å). The observed longer Si=Si distance in $\mathbf{6^{Br}}$ may be due to the significant intermolecular C–H···Br–C interaction in the crystals (H···Br distance: 3.08 Å) [31–34] (Figure 4). The substantial upfield-shifted ^{29}Si resonances of silyl-substituted double bond Si nuclei compared to that of aryl-substituted Si nuclei in **6** and $\mathbf{6^{Br}}$ (**6**: 74.9 (*Si*–$SiMe_3$) and 130.3 ppm (*Si*–anthryl); $\mathbf{6^{Br}}$: 75.1 (*Si*–$SiMe_3$) and 129.1 ppm (*Si*–anthryl)) have often been observed in 1-aryl-2-silyldisilenes [11,15,35].

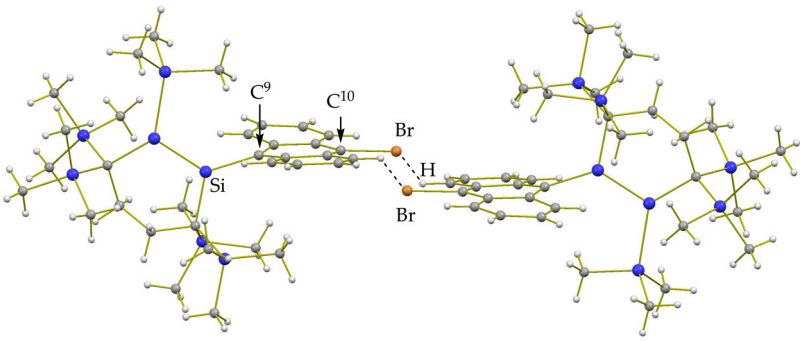

Figure 4. Crystal structure of $\mathbf{6^{Br}}$. The nearest Br···H distance is 3.08 Å and the Si–C^9–C^{10} angle is 164.7°.

1,2-Dianthryldisilene **7** also adopts a moderately *trans*-bent and slightly twisted geometry around the Si=Si double bond (bent angle β: 17.4° (Si1) and 21.0° (Si2); twist angle τ: 3.3°) (Figure 3e). The Si=Si distance of **7** (2.1525(7) Å) is shorter than those of disilenes **1**, **5**, **6** and $\mathbf{6^{Br}}$ probably due to the absence of the $SiMe_3$ group. The disilene π (π*Si*) and aromatic π (π*C*) systems in **7** are considerably twisted with respect to each other (dihedral angle δ: 79.7° (Si1) and 63.5° (Si2)). The upfield-shifted ^{29}Si resonance of this double bonded silicon nuclei in **7** (88.2 ppm) compared to that in **1** (131.4 ppm) is often observed in symmetrically-substituted silyl-substituted disilenes and aryl-substituted disilenes [1–3].

Similar to the reported anthryl-substituted disilenes [10,24,36], **6**, $\mathbf{6^{Br}}$, and **7** exhibit a weak and broad absorption band I assignable to π(Si=Si)→π*(anthryl) transition in the visible region as well as a structured intense band II that involves π(anthryl)→π*(anthryl) and π(Si=Si)→π*(Si=Si) transitions (300–400 nm). The absorption maximum of band I of **6** in hexane (535 nm (ε 9.3 × 10^2)) is slightly bathochromically shifted compared to that of trialkylanthryldisilene **B** (525 nm (ε 4.2 × 10^2)) (Figure 1) [10], which would be due to the presence of electron-donating silyl-substituents, while it is moderately hypsochromically shifted compared to triarylanthryldisilene **C** (550 nm (ε 3800)) [24]

(Figure 1) probably due to the absence of extra aryl groups. The maximum of band I of $\mathbf{6^{Br}}$ (578 nm) is considerably bathochromically shifted compared to that of **6**. The lower-lying π* orbitals in 10-bromo-9-anthryl group compared to 9-anthryl group may be responsible for the bathochromic shift of band I, which was qualitatively reproduced by density functional theory (DFT) calculations of **6** and $\mathbf{6^{Br}}$ (see, Figures S47 and S48). The absorption maximum of band I of 1,2-dianthryldisilene **7** (543 nm (1.68×10^3)) (Figure S49) is close to that of **6** and almost twice as large as that of **6**, which is consistent with the presence of two anthryl groups on the Si=Si double bond.

Two Si=Si double bonds in **8** are almost perpendicular to each other with the dihedral angle Si1–Si2–Si3–Si4 of 88.35(3)° (Figure 3f), which would be mainly due to the severe steric congestions around the central Si2–Si3 bond similar to the hitherto known tetrasila-1,3-dienes, such as Tip_2Si=SiTip–SiTip=$SiTip_2$ (**D**, dihedral angle: 51°) [25], ((t-$Bu_2MeSi)_2$Si=SiMes–SiMes=Si(Sit-$Bu_2Me)_2$) (**E**, 72(2)°) [12]), and R_2Si=Si($SiMe_3$)–Si($SiMe_3$)=SiR_2 (R_2 = 1,1,4,4-tetrakis(trimethylsilyl)butan-1,4-diyl) (**F**, 122.56(7)°) [26] (Figure 1). Each Si=Si double bond in **8** adopts a planar structure with the bent angles of 0.3–2.4°. While the Si2–Si3 distance (2.3392(5) Å) falls in the typical range of the Si–Si single bond, the Si=Si bond lengths of Si1–Si2 and Si3–Si4 in **8** (2.1850(5) and 2.1914(5) Å, respectively) are slightly longer than that of **1** (2.1762(5) Å). The ultraviolet-visible (UV-vis) absorption spectrum of **8** exhibits an intense and broad absorption band (437 nm (ε 3.42 × 10^4)) (Figure 5) accompanied by a shoulder peak at around 500 nm (ε 3.57 × 10^3). These bands are substantially bathochromically shifted compared to that of monodisilene **1** [420 (ε 1.57 × 104)], which suggests significant interactions between two Si=Si double bonds in **8**. DFT calculation provided further information on the interactions between two Si=Si double bonds in **8**. The optimized structure of **8** ($\mathbf{8_{opt}}$) at the B3PW91-D3/6-31G(d) level of theory is roughly consistent with the structure obtained from XRD analysis: the dihedral angle of two Si=Si bond of $\mathbf{8_{opt}}$ is 71.4° and the Si=Si distances are 2.1904 and 2.1907 Å. Even though the dihedral angle between the two Si=Si double bonds is large, the frontier orbitals involve two split π orbitals delocalized over two Si=Si double bonds (−4.61 and −4.79 eV at the B3LYP/6-311G(d)//B3PW91-D3/6-31G(d) level of theory), while LUMO and LUMO+1 correspond to π* orbitals (−1.75 and −1.46 eV). Time-dependent (TD) DFT calculation at the same level predicted four π→π* transitions, which is qualitatively consistent with the observed absorption bands of **8** (Figure S50). These results are consistent with a recent theoretical study that two Si=Si in tetrasila-1,3-diene can interact each other even at the dihedral angle of 90° due to the intrinsic non-planar geometry around the Si=Si double bond [16]. The longest wavelength absorption bands found in **8** (~500 nm) are hypsochromically-shifted compared those of the reported aryl-substituted tetrasila-1,3-dienes **D** (518 nm) [25], **E** (531 nm) [12] probably due to the absence of aryl-substituents, but close to that of structurally similar tetrasila-1,3-diene **F** (510 nm) [26] (Figure 1). The ^{29}Si resonances of **8** (106.4 (–*Si*=SiSiMe_3) and 143.0 ppm (–Si=*Si*SiMe_3)), which are upfield- and downfield-shifted compared to that of **1** (131.4 ppm), may also be consistent with the substantial interactions between two Si=Si double bonds.

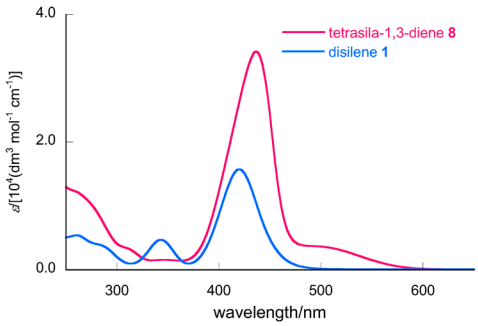

Figure 5. Ultraviolet–Visible absorption spectra of **1** and **8** in hexane.

3. Materials and Methods

3.1. General Procedure

All reactions involving air-sensitive compounds were performed under a nitrogen atmosphere using a high-vacuum line and standard Schlenk techniques, or a glove box, as well as dry and oxygen-free solvents. NMR spectra were recorded on a Bruker Avance 500 FT NMR spectrometer (Bruker Japan, Yokohama, Japan). The ^{1}H and ^{13}C NMR chemical shifts were referenced to residual ^{1}H and ^{13}C signals of the solvents: benzene-d_6 (^{1}H: δ 7.16 and ^{13}C: δ 128.0). The ^{29}Si NMR chemical shifts were relative to Me_4Si (δ 0.00). Sampling of air-sensitive compounds was carried out using a VAC NEXUS 100027 type glove box (Vacuum Atmospheres Co., Hawthorne, CA, USA). UV–Vis spectra were recorded on a JASCO V-660 spectrometer (JASCO, Tokyo, Japan). Melting points were measured on a SRS OptiMelt MPA100 (SRS, Sunnyvale, CA, USA) without correction.

3.2. Materials

Hexane, toluene and THF were dried using a VAC solvent purifier 103991 (Vacuum Atmospheres Co., Hawthorne, CA, USA). Benzene and 1,2-dimethoxyethane (DME) were dried over $LiAlH_4$, and then distilled under reduced pressure prior to use via a vacuum line. Benzene-d_6 and 1,2-dibromoethane were degassed and dried over 4A molecular sieves (activated). $CDCl_3$ was dried over 4A molecular sieves (activated). Potassium graphite (KC_8) [37] and Me_3SiSiH_2Ph [38] were prepared according to the procedure described in the literature. Bromine, 9-bromoanthracene, 9,10-dibromoanthracene, chlorotriethylsilane, lithium, magnesium sulfate (anhydrous), potassium *t*-butoxide (*t*-BuOK), Et_3N·HCl salt and triflic acid (TfOH) were purchased from commercial sources and used without further purification.

3.3. Preparation of 1,4-Bis(2,2,2-trimethyldisilanyl)-1,1,4,4-tetrakis(trimethylsilyl)butane **2**

In a Schlenk flask (200 mL) equipped with a magnetic stir bar, Me_3SiSiH_2Ph (15.5 g, 0.0859 mol) and hexane (30 mL) were placed. To the solution, TfOH (12.9 g, 0.0895 mol) was added at 0 °C. After stirring for 30 min, the reaction mixture was transferred to an another Schlenk flask (200 mL) equipped with a magnetic stir bar and Et_3N·HCl salt (28.3 g, 0.206 mol). After stirring for 30 min at room temperature, the resulting insoluble materials were removed by filtration. To the solution, a THF solution (100 mL) of $(Li(Me_3Si)_2CCH_2)_2\cdot(thf)_5$ (24.7 g, 0.0343 mmol), which was prepared from 1,1-bis(trimethylsilyl)ethene (11.9 g, 0.0690 mmol) and lithium (722 mg, 0.104 mmol) in THF [39], was added at −30 °C. After the mixture was stirred for 30 min, the resulting solution was hydrolyzed and extracted with hexane. The organic layer was separated, washed with a brine, dried over anhydrous magnesium sulfate, and finally concentrated under reduced pressure. Kugelrohr distillation (115 °C, 0.1 Pa) of the residue furnished 1,4-bis(2,2,2-trimethydisilanyl)-1,1,4,4-tetrakis(trimethylsilyl)butane (**2**) as a colorless oil (16.8 g, 0.305 mmol) in 89% yield.

2: a colorless oil; b.p. 115 °C/0.1 Pa (Kugelrohr); ^{1}H NMR ($CDCl_3$, 500 MHz, 300 K) δ 0.14 (s, 36H, Si(CH_3)$_3$), 0.22 (s, 18H, Si(CH_3)$_3$), 1.94 (s, 4H, CH_2), 3.51 (s, 4H, SiH_2); ^{13}C NMR ($CDCl_3$, 125 MHz, 300 K) δ 0.9 (Si(CH_3)$_3$), 1.8 ((Si(CH_3)$_3$), 3.8 (*C*), 32.5 (CH_2); ^{29}Si NMR ($CDCl_3$, 99 MHz, 301 K) δ −54.5 (SiH_2), −15.6 ($SiMe_3$), 3.2 ($SiMe_3$); MS (EI, 70 eV) *m*/*z* (%) 535.0 (15, M^+ − Me), 477.0 (41, M^+ − $SiMe_3$), 402.0 (76, M^+ − 2H − 2$SiMe_3$); Anal. Calcd. for $C_{22}H_{62}Si_8$: C, 47.92; H, 11.33; found: C, 47.84; H, 11.33%.

3.4. Preparation of 1,4-Bis(1,1-dibromo-2,2,2-trimethyldisilanyl)-1,1,4,4-tetrakis(trimethylsilyl)butane **3**

In a two-necked flask (100 mL), **2** (1.00 g, 1.81 mmol) and benzene (20 mL) were placed. To the mixture, bromine (1.19 g, 7.44 mmol) was added dropwise at 0 °C and then the mixture was stirred for 30 min at room temperature. The volatiles were removed in vacuo, and washing the residue with hexane afforded pure **3** as colorless crystals (1.09 g, 1.26 mmol) in 70% yield.

3: colorless crystals; m.p. 212 °C; ^{1}H NMR (C_6D_6, 500 MHz, 296 K) δ 0.36 (s, 18H, Si(CH_3)$_3$), 0.44 (s, 36H, Si(CH_3)$_3$), 2.74 (s, 4H, CH_2); ^{13}C NMR (C_6D_6, 125 MHz, 297 K) δ 0.4 (SiMe_3), 4.5 (SiMe_3), 19.2 (*C*), 32.6 (*C*H$_2$); ^{29}Si NMR (C_6D_6, 99 MHz, 296 K) δ −4.3 (*Si*Me$_3$), 2.5 (*Si*Me$_3$), 28.6 (*Si*Br$_2$); MS (EI, 70 eV) *m*/*z* (%) 851.0 (31, M$^+$ − Me), 641.0 (100, M$^+$ − 2SiMe$_3$ − Br), 560.0 (23, M$^+$ − 2SiMe$_3$ − 2Br), 487.0 (77, M$^+$ − 3SiMe$_3$ − 2Br); Anal. Calcd. for $C_{22}H_{58}Br_4Si_8$: C, 30.48; H, 6.74%. Found: C, 30.61; H, 6.95%.

3.5. Synthesis of 1,2,3,3,6,6-Hexakis(trimethylsilyl)-1,2-disilacyclohexene **1**

All operations were carried out in a glove box. In a Schlenk tube (50 mL), **3** (1.26 g, 1.45 mmol), KC_8 (825 mg, 6.10 mmol) and THF (70 mL) were placed. After stirring the mixture at room temperature for three hours, the volatiles were removed under reduced pressure. Then dry hexane was added to the residue and the resulting salt was filtered off. Removal of hexane under reduced pressure gave disilene **1** as yellow crystals (789.0 mg, 1.44 mmol) in 99% yield.

1: yellow crystals; m.p. 120 °C; ^{1}H NMR (C_6D_6, 500 MHz, 296 K) δ 0.25 (s, 18H, Si(CH_3)$_3$), 0.34 (s, 18H, Si(CH_3)$_3$), 0.47 (s, 18H, Si(CH_3)$_3$), 1.90–2.00 (m, 2H, CH_2), 2.45–2.57 (m, 2H, CH_2); ^{13}C NMR (C_6D_6, 125 MHz, 297 K) δ 1.1 (Si(*C*H$_3$)$_3$), 4.32 (Si(*C*H$_3$)$_3$), 4.34 (Si(*C*H$_3$)$_3$), 20.7 (*C*), 34.5 (*C*H$_2$); ^{29}Si NMR (C_6D_6, 99 MHz, 296 K) δ −11.9 (*Si*Me$_3$), 0.8 (*Si*Me$_3$), 1.6 (*Si*Me$_3$), 131.4 (*Si*=*Si*); UV–Vis (hexane, room temperature) λ_{max}/nm (ε) 420 (1.57×10^4), 343 (4.63×10^3); HRMS (APCI) *m*/*z* [M]$^+$ Calcd. for $C_{22}H_{58}Si_8$: 546.2687. Found. 546.2687; Anal. Calcd. for $C_{22}H_{58}Si_8$: C, 48.27; H, 10.68%. Found: C, 48.21; H, 10.55%.

3.6. Synthesis of Potassium 2,3,3,6,6-Pentakis(trimethylsilyl)-1,2-disilacyclohexen-1-ide **4**

In a Schlenk tube (50 mL) equipped with a magnetic stir bar, disilene **1** (81.4 mg, 0.149 mmol) and *t*-BuOK (17.6 mg, 0.157 mmol) and THF (9.0 mL) were placed. After stirring for one hour at room temperature, disilenide **4** was formed as a sole product, which was confirmed by NMR spectroscopy. The volatiles including THF and the resulting *t*-BuOSiMe$_3$ were removed under reduced pressure and then the resulting residue was washed with hexane to afford **4**(thf) as an orange powder (43.0 mg, 7.35×10^{-2} mmol) in 49% yield.

4(thf): an orange powder; m.p. 157 °C; ^{1}H NMR (C_6D_6, 500 MHz, 323 K) δ 0.33 (s, 27H, 3 × Si(CH_3)$_3$), 0.47 (s, 9H, Si(CH_3)$_3$), 0.49 (s, 9H, Si(CH_3)$_3$), 1.43–1.45 (m, 4H, 2 × CH_2 of THF), 2.15–2.24 (m, 2H, CH_2), 2.69–2.83 (m, 2H, CH_2), 3.54–3.56 (m, 4H, 2 × CH_2 of THF); ^{13}C NMR (C_6D_6, 125 MHz, 323 K) δ 1.9 (Si(*C*H$_3$)$_3$), 2.1 (Si(*C*H$_3$)$_3$), 4.6 (Si(*C*H$_3$)$_3$), 5.1 (Si(*C*H$_3$)$_3$), 6.4 (Si(*C*H$_3$)$_3$), 20.8 (*C*), 24.2 (*C*), 33.6 (*C*H$_2$), 35.2 (*C*H$_2$), 25.9 (*C*H$_2$ in THF), 68.0 (*C*H$_2$ in THF); ^{29}Si NMR (C_6D_6, 99 MHz, 323 K) δ −15.9 (*Si*Me$_3$), −3.1 (*Si*Me$_3$), −2.9 (*Si*Me$_3$), −2.3 (*Si*Me$_3$), −1.4 (*Si*Me$_3$), 146.9 (=*Si*SiMe$_3$), 219.3 (=*Si*$^-$). The elemental analysis was unsuccessful as **4**(thf) is very sensitive to air and moisture.

Similar to the reaction in THF, **4**(dme) (63.2 mg, 9.11×10^{-2} mmol, 49% yield) was obtained from **1** (102 mg, 1.86×10^{-1} mmol), *t*-BuOK (22.5 mg, 2.0×10^{-1} mmol) and DME (9.0 mL).

4(dme): an orange powder; m.p. 135 °C; ^{1}H NMR (C_6D_6, 500 MHz, 323 K) δ 0.37 (s, 9H, 2 × Si(CH_3)$_3$), 0.39 (s, 9H, Si(CH_3)$_3$), 0.49 (s, 9H, Si(CH_3)$_3$), 0.54 (s, 9H, Si(CH_3)$_3$), 2.24–2.30 (m, 2H, CH_2), 2.70–2.87 (m, 2H, CH_2), 3.05 (s, 6H, 2 × CH_3O of DME), 3.07 (s, 2H, OCH_2CH_2O), 3.08 (s, 2H, OCH_2CH_2O of DME); ^{13}C NMR (C_6D_6, 125 MHz, 323 K) δ 1.9 (Si(*C*H$_3$)$_3$), 2.1 (Si(*C*H$_3$)$_3$), 4.6 (Si(*C*H$_3$)$_3$), 5.0 (Si(*C*H$_3$)$_3$), 6.3 (Si(*C*H$_3$)$_3$), 33.6 (*C*H$_2$), 35.1 (*C*H$_2$), 58.9 (*C*H$_3$O of DME), 71.6 (OCH_2CH_2O in DME), 71.7 (OCH_2CH_2O of DME); ^{29}Si NMR (C_6D_6, 99 MHz, 323 K) δ −15.9 (*Si*Me$_3$), −3.2 (*Si*Me$_3$), −2.3 (*Si*Me$_3$), −1.5 (*Si*Me$_3$), 142.9, 143.1 (=*Si*SiMe$_3$), 222.2 (=*Si*$^-$). The reasons for the observation of very slightly split signals that can be assigned to one of the double bonded Si nuclei remain unclear at this point.

3.7. Synthesis of 1-Triethylsilyl-2,3,3,6,6-pentakis(trimethylsilyl)-1,2-disilacyclohexene **5**

In a Schlenk tube (50 mL) equipped with a magnetic stir bar, disilene **1** (450.0 mg, 0.822 mmol), *t*-BuOK (92.2 mg, 0.822 mmol) and THF (8 mL) were placed. After stirring for one hour at room temperature, disilenide **4** was formed quantitatively, which was confirmed by NMR spectroscopy.

Then, THF was removed in vacuo. To the residue toluene (10 mL) and chlorotriethylsilane (150.0 mg, 0.995 mmol) were added. After stirring for 15 min at room temperature, the volatiles were removed in vacuo. To the residue dry hexane was added and the resulting salt was filtered off. Removal of hexane from the filtrate gave Et_3Si-substituted disilene **5** as yellow crystals (481 mg, 0.816 mmol) in 99% yield.

5: yellow crystals; m.p. 180 °C; ^{1}H NMR (C_6D_6, 500 MHz) δ 0.270 (s, 9H, Si(CH_3)$_3$), 0.273 (s, 9H, Si(CH_3)$_3$), 0.35 (s, 9H, Si(CH_3)$_3$), 0.37 (s, 9H, Si(CH_3)$_3$), 0.48 (s, 9H, Si(CH_3)$_3$), 0.94–1.09 (m, 6H, Si(CH_2CH$_3$)$_3$), 1.17 (t, *J* = 7.8 Hz, 9H, Si(CH$_2$CH_3)$_3$), 1.88–2.02 (m, 2H, CH_2), 2.49–2.62 (m, 2H, CH_2); ^{13}C NMR (C_6D_6, 125 MHz, 300 K) δ 1.01 (Si(CH_3)$_3$), 1.03 (Si(CH_3)$_3$), 4.1 (Si(CH_3)$_3$), 4.3 (Si(CH_3)$_3$), 4.4 (Si(CH$_3$)$_3$), 7.8 (Si(CH$_2$CH_3)$_3$), 9.2 (Si(CH$_2$CH_3)$_3$), 20.7 (CH_2), 21.3 (CH_2), 34.5 (*C*), 34.9 (*C*); ^{29}Si NMR (C_6D_6, 99 MHz, 300 K) δ −12.5 (*Si*Me$_3$), 0.4 (SiMe$_3$), 0.5 (SiMe$_3$), 1.0 (*Si*Et$_3$), 1.3 (*Si*Me$_3$), 1.8 (*Si*Me$_3$), 123.5 (Et$_3$Si*Si*=), 134.2 (Me$_3$Si*Si*=); HRMS (APCI) *m*/*z* [M]$^+$ Calcd. for $C_{25}H_{64}Si_8$: 588.3157, Found. 588.3156; Anal. Calcd. for $C_{25}H_{64}Si_8$: C, 50.94; H, 10.94%. Found: C, 50.58; H, 10.70.

3.8. Synthesis of 1-(9-Anthryl)-2,3,3,6,6-pentakis(trimethylsilyl)-1,2-disilacyclohexene **6**

In a Schlenk tube (50 mL) equipped with a magnetic stir bar, disilene **1** (181 mg, 3.30×10^{-1} mmol) and *t*-BuOK (38.0 mg, 3.39×10^{-1} mmol) and DME (15.0 mL) were placed. After stirring for one hour at room temperature, disilenide **4** was formed as a sole product, which was confirmed by NMR spectroscopy. Then DME was removed in vacuo, and the resulting residue was dissolved in benzene (11.0 mL). To the solution, a benzene solution (7.5 mL) of 9-bromoanthracene (86.2 mg, 3.35×10^{-1} mmol) was added and the mixture was stirred for 1 min at room temperature. The resulting salt was removed by filtration and washed with benzene and the solvent was removed from the filtrate in vacuo. Formation of the anthryl-substituted disilene **6** as a major product was observed by ^{1}H NMR spectrum. Recrystallization from hexane and DME at −35 °C gave **6** as reddish purple crystals (83.6 mg, 1.28×10^{-1} mmol) in 33% yield.

6: reddish purple crystals; m.p. 178 °C; ^{1}H NMR (C_6D_6, 500 MHz, 298 K) δ −0.21 (s, 9H, Si(CH_3)$_3$), −0.01 (s, 9H, Si(CH_3)$_3$), 0.32 (s, 9H, Si(CH_3)$_3$), 0.40 (s, 9H, Si(CH_3)$_3$), 0.48 (s, 9H, Si(CH_3)$_3$), 2.34–2.45 (m, 1H, CH$_2$CH*H*), 2.52–2.59 (m, 3H, CH$_2$C*H*H), 7.21–7.24 (m, 2H, 2 × C*H*), 7.37–7.42 (m, 2H, 2 × C*H*), 7.72–7.76 (m, 2H, 2 × C*H*), 8.19 (s, 1H, C*H*), 9.45 (d, *J* = 8.7 Hz, 1H, C*H*), 9.75 (d, *J* = 8.8 Hz, 1H, C*H*); ^{13}C NMR (C_6D_6, 125 MHz, 298 K) δ 1.68 (Si(CH_3)$_3$), 1.73 (Si(CH_3)$_3$), 3.1 (Si(CH_3)$_3$), 3.6 (Si(CH_3)$_3$), 4.5 (Si(CH$_3$)$_3$), 15.0 (*C*), 23.6 (*C*), 32.3 (CH_2), 32.5 (CH_2), 125.2 (2 × *C*H), 125.5 (*C*H), 125.6 (*C*H), 129.46 (*C*H), 129.49 (*C*H), 131.0 (*C*H), 131.9 (*C*), 132.4 (*C*), 132.8 (*C*H), 133.7 (*C*H), 137.7 (*C*), 138.1 (*C*), 138.5 (*C*); ^{29}Si NMR (C_6D_6, 99 MHz, 297 K) δ −10.0 (*Si*Me$_3$), 1.6 (*Si*Me$_3$), 1.7 (*Si*Me$_3$), 2.2 (*Si*Me$_3$), 2.3 (*Si*Me$_3$), 74.9 (=*Si*(SiMe$_3$)), 130.3 (Ant*Si*=); UV–Vis (hexane) λ_{max}/nm (ε) 399 (26400), 535 (925); MS (EI, 70 eV) *m*/*z* (%) (682.0 (53, M$^+$ + O$_2$)), 650.0 (19, M$^+$), 577.0 (100, M$^+$ − SiMe$_3$); Anal. Calcd. for $C_{33}H_{58}Si_7$: C, 60.85; H, 8.970. Found: C, 60.69; H, 9.042%.

3.9. Synthesis of 1-(10-Bromo-9-anthryl)-2,3,3,6,6-pentakis(trimethylsilyl)-1,2-disilacyclohexene $\mathbf{6^{Br}}$

In a Schlenk tube (50 mL) equipped with a magnetic stir bar, were placed disilene **1** (169 mg, 3.08×10^{-1} mmol) and *t*-BuOK (36.0 mg, 3.21×10^{-1} mmol) and DME (6.0 mL). After stirring for one hour at room temperature, disilenide **4** was formed as a sole product, which was confirmed by NMR spectroscopy. Then DME was removed in vacuo and benzene (7.5 mL) was added. The resulting benzene solution of **4** was added to a benzene (17 mL) solution of 9,10-dibromoanthracene (103 mg, 3.06×10^{-1} mmol) in another Schlenk tube (50 mL) equipped with a magnetic stir bar. After the mixture was stirred for 1 min at room temperature, the resulting salt was removed by filtration and washed with benzene and the volatiles were removed from the filtrate in vacuo. Formation of 9-bromoanthryl-substituted disilene $\mathbf{6^{Br}}$ as a major product was observed by ^{1}H NMR spectrum. Recrystallization from hexane at –35 °C gave $\mathbf{6^{Br}}$ (32.0 mg, 4.38×10^{-2} mmol) as blue crystals in 14% yield including anthryldisilene **6** as a major contaminant. Further separation of **6** and $\mathbf{6^{Br}}$ was unsuccessful.

$\mathbf{6^{Br}}$ (including **6** (~10%)): blue crystals; ^{1}H NMR (C_6D_6, 500 MHz, 298 K) δ −0.26 (s, 9H, Si(CH_3)$_3$), −0.04 (s, 9H, Si(CH_3)$_3$), 0.27 (s, 9H, Si(CH_3)$_3$), 0.38 (s, 9H, Si(CH_3)$_3$), 0.45 (s, 9H, Si(CH_3)$_3$), 2.35–2.40

(m, 1H, C*H*HCH$_2$), 2.49–2.56 (m, 3H, CH*H*CH$_2$), 7.23–7.27 (m, 2H, 2 × C*H*), 7.30–7.35 (m, 2H, 2 × C*H*), 8.62 (d, *J* = 8.6, 1H, C*H*), 8.65 (dd, *J* = 8.7 Hz, 14.6 Hz, 1H, C*H*), 9.53 (d, *J* = 8.5 Hz, 1H, C*H*), 9.85 (d, *J* = 8.7 Hz, 1H, C*H*); ^{13}C NMR (C$_6$D$_6$, 125 MHz, 299 K) δ 1.65 (Si(CH$_3$)$_3$), 1.70 (Si(CH$_3$)$_3$), 3.07 (Si(CH$_3$)$_3$), 3.60 (Si(CH$_3$)$_3$), 4.44 (Si(CH$_3$)$_3$), 15.1 (*C*), 23.6 (*C*), 32.3 (CH$_2$) 32.4 (CH$_2$), 125.36 (*C*H), 125.38 (*C*H), 127.5 (*C*H), 127.6 (*C*H), 128.9 (*C*H), 129.0 (*C*H), 131.0 (*C*), 131.5 (*C*), 133.2 (*C*H), 134.2 (*C*H), 138.2 (*C*), 138.6 (*C*), 140.3 (*C*); ^{29}Si NMR (C$_6$D$_6$, 99 MHz, 298 K) δ −9.9 (*Si*Me$_3$), 1.7 (*Si*Me$_3$), 1.8 (*Si*Me$_3$), 2.29 (*Si*Me$_3$), 2.34 (*Si*Me$_3$), 75.1 (=*Si*(SiMe$_3$)), 129.1 [(BrAnt)*Si*=]; UV–Vis (hexane) λ_{max}/nm (ε) 391 (24800), 410 (30800), 578 (967); HRMS (APCI) *m*/*z* [M]$^+$ Calcd. for C$_{33}$H$_{57}$BrSi$_7$: 728.2029. Found. 728.2026; [M$^+$ + H$^+$]. for C$_{33}$H$_{58}$BrSi$_7$: 729.2107. Found: 729.2104; [M$^+$ − H$^+$] Calcd. for C$_{33}$H$_{56}$BrSi$_7$: 727.1950. Found: 727.1947. A quaternary carbon signal was not observed in the ^{13}C NMR spectrum.

3.10. Synthesis of 1,2-Di(9-anthryl)-3,3,6,6-tetrakis(trimethylsilyl)-1,2-disilacyclohexene **7**

In a Schlenk tube (50 mL) equipped with a magnetic stir bar, were placed **6** (38.7 mg, 7.07 ×10^{-2} mmol), *t*-BuOK (8.70 mg, 7.75 × 10^{-2} mmol) and DME (7.5 mL). After stirring for one hour at room temperature, the corresponding disilenide was formed as a sole product, as confirmed by NMR spectroscopy. Then the volatiles were removed in vacuo and benzene was added. To the solution, a benzene solution of 9-bromoanthracene (17.1 mg, 6.65 × 10^{-2} mmol) was added. The ^{1}H NMR spectrum of the reaction mixture indicated formation of the desired bisanthryl-substituted disilene. The resulting salt was removed by filtration and washed with benzene and the volatiles were removed from the filtrate in vacuo. Recrystallization from toluene at −35 °C gave disilene **7** as black purple crystals (7.50 mg, 9.93 × 10^{-3} mmol) in 17% yield.

7: black purple crystals; m.p. 220 °C (decomp.); ^{1}H NMR (C$_6$D$_6$, 500 MHz, 298 K) δ −0.11 (s, 18H, 2 × Si(C*H*$_3$)$_3$), 0.58 (s, 18H, 2 × Si(C*H*$_3$)$_3$), 2.81 (s, 4H, (C*H*$_2$)$_2$), 6.84–6.87 (m, 2H, 2 × C*H*), 7.10–7.14 (m, 2H, 2 × C*H*), 7.23–7.30 (m, 4H, 4 × C*H*), 7.55–7.58 (m, 4H, 4 × C*H*), 7.78 (s, 2H, 2 × C*H*), 9.57–9.59 (m, 2H, 2 × C*H*), 9.82–9.84 (m, 2H, 2 × C*H*); ^{13}C NMR (C$_6$D$_6$, 125 MHz, 299 K) δ 1.5 (Si(*C*H$_3$)$_3$), 4.6 (Si(*C*H$_3$)$_3$), 21.3 (*C*H$_2$), 32.6 (*C*), 125.06 (*C*H), 125.09 (*C*H), 125.14 (*C*H), 129.1 (*C*H), 129.7 (*C*H), 130.8 (*C*H), 131.7 (*C*), 132.3 (*C*), 132.6 (*C*H), 132.9 (*C*H), 136.2 (*C*), 137.6 (*C*), 137.7 (*C*); ^{29}Si NMR (C$_6$D$_6$, 99 MHz, 298 K) δ 2.6 (*Si*Me$_3$), 3.8 (*Si*Me$_3$), 88.2 (*Si*=*Si*); UV–Vis (hexane) λ_{max}/nm (ε) 340 (5250), 357 (8640), 375 (14100), 543 (1680); MS (EI, 70 eV) *m*/*z* (%) 755 (11, M$^+$), 681 (2.9, M$^+$ − SiMe$_3$), 607 (1.5, M$^+$ − 2SiMe$_3$); Anal. Calcd. for C$_{44}$H$_{58}$Si$_6$: C, 69.96; H, 7.74. Found: C, 68.54; H, 7.774%. Although the reason why the observed relative ratio of carbon atoms in the elemental analysis was less than the calculated value remains unclear at this point, flame resistant materials such as silicon carbide may be formed during elemental analysis.

3.11. Synthesis of 1,4-Bis(trimethylsilyl)tetrasila-1,3-diene **8**

In a Schlenk tube (50 mL) equipped with a magnetic stir bar, were placed disilene **1** (139.9 mg, 0.256 mmol), *t*-BuOK (29.0 mg, 0.258 mmol) and THF (5 mL). After the mixture was stirred for one hour at room temperature, ^{1}H NMR spectrum of the mixture showed that disilenide **4** was formed quantitatively. Then, to the mixture, 1,2-dibromoethane (24.0 mg, 0.128 mmol) was added at 0 °C. After additional stirring of the mixture for 15 min at 0 °C, the volatiles were removed under reduced pressure. To the residue dry hexane was added and the resulting insoluble materials were filtered off. Removal of hexane from the filtrate and subsequent recrystallization from diethyl ether at −35 °C gave tetrasila-1,3-diene **8** as red crystals (104.0 mg, 0.110 mmol) in 86% yield.

8: red crystals; m.p. 220 °C (decomp.); ^{1}H NMR (C$_6$D$_6$, 500 MHz, 296 K) δ 0.30 (s, 18H, Si(C*H*$_3$)$_3$), 0.37 (s, 18H, Si(C*H*$_3$)$_3$), 0.468 (s, 18H, Si(C*H*$_3$)$_3$), 0.470 (s, 18H, Si(C*H*$_3$)$_3$), 0.68 (s, 18H, Si(C*H*$_3$)$_3$), 2.06–2.15 (m, 4H, C*H*$_2$), 2.45–2.64 (m, 4H, C*H*$_2$); ^{13}C NMR (C$_6$D$_6$, 125 MHz, 296 K) δ 1.8 (Si(*C*H$_3$)$_3$), 3.2 (Si(*C*H$_3$)$_3$), 4.8 (Si(*C*H$_3$)$_3$), 5.66 (Si(*C*H$_3$)$_3$), 5.74 (Si(*C*H$_3$)$_3$), 23.5 (*C*), 26.9 (*C*), 33.5 (*C*H$_2$), 36.7 (*C*H$_2$); ^{29}Si NMR (C$_6$D$_6$, 99 MHz, 296 K) δ −10.9 (*Si*Me$_3$), 1.4 (*Si*Me$_3$), 2.8 (*Si*Me$_3$), 3.3 (*Si*Me$_3$), 3.6 (*Si*Me$_3$), 106.4 (*Si*=SiSiMe$_3$), 143.0 (Si=*Si*SiMe$_3$); UV–Vis (hexane, room temperature) λ_{max}/nm (ε) ~500 (sh,

3.57 × 10^3), 437 (3.42 × 10^4); HRMS (APCI) m/z $[M]^+$ Calcd. for $C_{38}H_{98}Si_{14}$: 946.4433. Found. 946.4430; Anal. Calcd. for $C_{38}H_{98}Si_{14}$: C, 48.13; H, 10.42%. Found: C, 48.48; H, 10.58%.

3.12. Single Crystal X-ray Diffraction Analyses

Single crystals for data collection were obtained by recrystallization under the following conditions: from hexane at −35 °C (**1**, **5, 6**, $\mathbf{6^{Br}}$), from toluene at −35 °C ((**4**(toluene))$_2$, **7**) or from diethyl ether at −35 °C (**8**). Each single crystal coated by Apiezon® grease was mounted on the glass fiber and transferred to the cold nitrogen gas stream of the diffractometer. X-ray data were collected on a BrukerAXS APEXII diffractometer with graphite monochromated Mo-Kα radiation (λ = 0.71073 Å). The data were corrected for Lorentz and polarization effects. An empirical absorption correction based on the multiple measurement of equivalent reflections was applied using the program SADABS [40]. The structures were solved by direct methods and refined by full-matrix least squares against F^2 using all data (SHELXL-2014/7) [41]. CCDC-1813641–1813647 contain the supplementary crystallographic data for this paper. These data can be obtained free of charge via http://www.ccdc.cam.ac.uk/conts/retrieving.html (or from the CCDC, 12 Union Road, Cambridge CB2 1EZ, UK; Fax: +44-1223-336033; E-mail: deposit@ccdc.cam.ac.uk).

1: CCDC-1813641; 100 K; $C_{22}H_{58}Si_8$; Fw 547.40; orthorhombic; space group P_{bca} (#61); a = 17.3380(16) Å, b = 18.0108(16) Å, c = 22.317(2) Å, V = 6969.0(11) Å^3, Z = 8, D_{calcd} = 1.043 Mg/m^3, $R1$ = 0.0218 ($I > 2\sigma(I)$), $wR2$ = 0.0619 (all data), GOF = 1.051.

4: CCDC-1813642; 100 K; $C_{26}H_{57}KSi_7$; Fw 605.45; monoclinic; space group $P2_1/n$ (#14), a = 15.7323(17) Å, b = 11.7003(13) Å, c = 21.031(2) Å, β = 107.1880(10)°, V = 3698.4(7) Å^3, Z = 4, D_{calcd} = 1.087 Mg/m^3, $R1$ = 0.0234 ($I > 2\sigma(I)$), $wR2$ = 0.0642 (all data), GOF = 1.049.

5: CCDC-1813643; 100 K; $C_{25}H_{64}Si_8$; Fw 589.48; monoclinic; space group $P2_1/n$ (#14), a = 9.0608(19) Å, b = 37.640(8) Å, c = 11.263(2) Å, β = 103.230(2)°, V = 3739.3(14) Å^3, Z = 4, D_{calcd} = 1.047 Mg/m^3, $R1$ = 0.0729 ($I > 2\sigma(I)$), $wR2$ = 0.1806 (all data), GOF = 1.335.

6: CCDC-1813644; 100 K; $C_{33}H_{58}Si_7$; Fw 651.42; monoclinic; space group $P2_1/c$ (#14), a = 17.7493(8) Å, b = 9.0323(4) Å, c = 23.7624(10) Å, β = 91.2830(10)°, V = 3808.6(3) Å^3, Z = 4, D_{calcd} = 1.136 Mg/m^3, $R1$ = 0.0320 ($I > 2\sigma(I)$), $wR2$ = 0.0847 (all data), GOF = 1.038.

$\mathbf{6^{Br}}$: CCDC-1813645; 100 K; $C_{33}H_{57}BrSi_7$; Fw 730.32; triclinic; space group *P-1* (#2), a = 9.0529(3) Å, b = 11.9109(4) Å, c = 19.1793(7) Å, α = 93.9480(10)°, β = 90.1810(10)°, γ = 109.1330(10)°, V = 1947.47(12) Å^3, Z = 2, D_{calcd} = 1.245 Mg/m^3, $R1$ = 0.0263 ($I > 2\sigma(I)$), $wR2$ = 0.0701 (all data), GOF = 1.043.

7: CCDC-1813646; 100 K; $C_{44}H_{58}Si_6 \cdot C_7H_8$; Fw 847.57; triclinic; space group *P-1* (#2), a = 11.0302(9) Å, b = 12.8081(10) Å, c = 15.7049(13) Å, α = 95.628(2)°, β = 98.481(2)°, γ = 90.755(2)°, V = 2361.1(3) Å^3, Z = 2, D_{calcd} = 1.192 Mg/m^3, $R1$ = 0.0350 ($I > 2\sigma(I)$), $wR2$ = 0.0954 (all data), GOF = 1.025.

8: CCDC-1813647; 173 K; $C_{38}H_{98}Si_{14}$; Fw 948.42; triclinic; space group *P-1* (#2), a = 11.4093(11) Å, b = 15.6821(15) Å, c = 19.5623(19) Å, α = 84.8020(10)°, β = 75.9110(10)°, γ = 71.9750(10)°, V = 3227.8(5) Å^3, Z = 2, D_{calcd} = 0.976 Mg/m^3, $R1$ = 0.0266 ($I > 2\sigma(I)$), $wR2$ = 0.0759 (all data), GOF = 1.039.

4. Conclusions

We successfully synthesized 1,2-bis(trimethylsilyl)-1,2-disilacyclhexene **1** and converted the silyl group(s) to the functional group(s). Noticeably, two silyl groups in **1** can be replaced stepwise by anthryl groups, which suggests that **1** can serve as a unit of *cis*-1,2-dialkyldisilene for novel extended π-electron systems. As the introduction of heteroatoms into sp^2-carbon-based nanocarbon materials such as polycyclic aromatic hydrocarbons, fullerenes and graphenes has received substantial attention, nanocarbon materials in which the Si=Si double bond was introduced into the peripheral position by using functionalizable disilenes such as **1** may provide novel, fascinating nanosilicon–carbon hybrid materials.

Supplementary Materials: The following are available online at www.mdpi.com/2304-6740/6/1/21/s1, Figures S1–S45: NMR spectra of **1**–**8**, Figures S46–S50: UV–Vis spectra of **1**, **6**, $\mathbf{6^{Br}}$, **7**, **8**, Tables S1–S5: Transition Energy, Wavelength, and Oscillator Strengths of the Electronic Transition of **1**, **6**, $\mathbf{6^{Br}}$, **7**, **8**, Table S6: Selected structures of **1**, **6**, $\mathbf{6^{Br}}$, **7**, **8** optimized at the B3PW91-D3/6-31G(d) level of theory and a xyz file for the optimized structures of **1**, **6**, $\mathbf{6^{Br}}$, **7**, **8**.

Acknowledgments: This work was supported by JSPS KAKENHI grant JP24655024, JPK1513634 (Takeaki Iwamoto), and Grant-in-Aid for JSPS Fellows (Naohiko Akasaka).

Author Contributions: Naohiko Akasaka, Kaho Tanaka and Takeaki Iwamoto conceived and designed the experiments; Naohiko Akasaka and Kaho Tanaka performed the experiments; Shintaro Ishida, Naohiko Akasaka and Takeaki Iwamoto performed the X-ray single crystal analyses; Naohiko Akasaka, Kaho Tanaka and Takeaki Iwamoto analyzed the NMR data; Takeaki Iwamoto performed theoretical calculations; Naohiko Akasaka, Kaho Tanaka and Takeaki Iwamoto wrote the manuscript.

Conflicts of Interest: The authors declare no conflict of interest.

References

1. Okazaki, R.; West, R. Chemistry of stable disilenes. *Adv. Organomet. Chem.* **1996**, *39*, 231–273.
2. Kira, M.; Iwamoto, T. Progress in the chemistry of stable disilenes. *Adv. Organomet. Chem.* **2006**, *54*, 73–148.
3. Lee, V.Y.; Sekiguchi, A. Heavy analogs of alkenes, 1,3-dienes, allenes and alkynes: Multiply bonded derivatives of Si, Ge, Sn and Pb. In *Organometallic Compounds of Low-Coordinate Si, Ge, Sn and Pb: From Phantom Species to Stable Compounds*; Wiley-VCH: Chichester, Germany, 2010; pp. 199–334.
4. Scheschkewitz, D. Anionic reagents with silicon-containing double bonds. *Chem. Eur. J.* **2009**, *15*, 2476–2485. [CrossRef] [PubMed]
5. Abersfelder, K.; Scheschkewitz, D. Synthesis of homo- and heterocyclic silanes via intermediates with Si=Si bonds. *Pure Appl. Chem.* **2010**, *82*, 595–602. [CrossRef]
6. Scheschkewitz, D. The versatile chemistry of disilenides: Disila analogues of vinyl anions as synthons in low-valent silicon chemistry. *Chem. Lett.* **2011**, *40*, 2–11. [CrossRef]
7. Präsang, C.; Scheschkewitz, D. Silyl anions. *Struct. Bonding* **2013**, *156*, 1–47.
8. Präsang, C.; Scheschkewitz, D. Reactivity in the periphery of functionalised multiple bonds of heavier group 14 elements. *Chem. Soc. Rev.* **2016**, *45*, 900–921. [CrossRef] [PubMed]
9. Rammo, A.; Scheschkewitz, D. Functional disilenes in synthesis. *Chem. Eur. J.* **2017**. [CrossRef] [PubMed]
10. Iwamoto, T.; Kobayashi, M.; Uchiyama, K.; Sasaki, S.; Nagendran, S.; Isobe, H.; Kira, M. Anthryl-substituted trialkyldisilene showing distinct intramolecular charge-transfer transition. *J. Am. Chem. Soc.* **2009**, *131*, 3156–3157. [CrossRef] [PubMed]
11. Scheschkewitz, D. A silicon analogue of vinyllithium: Structural characterization of a disilenide. *Angew. Chem. Int. Ed.* **2004**, *43*, 2965–2967. [CrossRef] [PubMed]
12. Ichinohe, M.; Sanuki, K.; Inoue, S.; Sekiguchi, A. Disilenyllithium from tetrasila-1,3-butadiene: A silicon analogue of a vinyllithium. *Organometallics* **2004**, *23*, 3088–3090. [CrossRef]
13. Ichinohe, M.; Sanuki, K.; Inoue, S.; Sekiguchi, A. Tetrasila-1,3-butadiene and its transformation to disilenyl anions. *Silicon Chem.* **2006**, *3*, 111–116. [CrossRef]
14. Meltzer, A.; Majumdar, M.; White, A.J.P.; Huch, V.; Scheschkewitz, D. Potential protecting group strategy for disila analogues of vinyllithiums: Synthesis and reactivity of a 2,4,6-trimethoxyphenyl-substituted disilene. *Organometallics* **2013**, *32*, 6844–6850. [CrossRef]
15. Abersfelder, K.; Zhao, H.; White, A.J.P.; Präsang, C.; Scheschkewitz, D. Synthesis of the first homoleptic trisilaallyl chloride: 3-Chloro-1,1,2,3,3-pentakis(2′,4′,6′-triisopropylphenyl)trisil-1-ene. *Z. Anorg. Allg. Chem.* **2015**, *641*, 2051–2055. [CrossRef]
16. Akasaka, N.; Fujieda, K.; Garoni, E.; Kamada, K.; Matsui, H.; Nakano, M.; Iwamoto, T. Synthesis and functionalization of a 1,4-bis(trimethylsilyl)tetrasila-1,3-diene through the selective cleavage of Si(sp^2)-Si(sp^3) bonds under mild reaction conditions. *Organometallics* **2018**, *37*, 172–175. [CrossRef]
17. Marschner, C. Silicon-centered anions. In *Organosilicon Compounds Theory and Experiment (Synthesis)*; Lee, V.Y., Ed.; Academic Press: Oxford, UK, 2017; pp. 295–360.
18. Abe, T.; Iwamoto, T.; Kira, M. A stable 1,2-disilacyclohexene and its 14-electron palladium(0) complex. *J. Am. Chem. Soc.* **2010**, *132*, 5008–5009. [CrossRef] [PubMed]

19. Liang, C.; Allen, L.C. Group IV double bonds: Shape deformation and substituent effects. *J. Am. Chem. Soc.* **1990**, *112*, 1039–1041. [CrossRef]
20. Karni, M.; Apeloig, Y. Substituent effects on the geometries and energies of the Si=Si double bond. *J. Am. Chem. Soc.* **1990**, *112*, 8589–8590. [CrossRef]
21. Apeloig, Y.; Müller, T. Do silylenes always dimerize to disilenes? Novel silylene dimers with unusual structures. *J. Am. Chem. Soc.* **1995**, *117*, 5363–5364. [CrossRef]
22. Goldberg, D.E.; Hitchcock, P.B.; Lappert, M.F.; Thomas, K.M.; Thorne, A.J.; Fjeldberg, T.; Haaland, A.; Schilling, B.E.R. Subvalent Group 4B metal alkyls and amides. Part 9. Germanium and tin alkene analogues, the dimetallenes M_2R_4[M = Ge or Sn, R = $CH(SiMe_3)_2$]: X-ray structures, molecular orbital calculations for M_2H_4, and trends in the series $M_2R'_4$[M = C, Si, Ge, or Sn; R′ = R, Ph, $C_6H_2Me_3$-2,4,6, or $C_6H_3Et_2$-2,6]. *J. Chem. Soc. Dalton Trans.* **1986**, 2387–2394.
23. West, R.; Cavalieri, J.D.; Buffy, J.J.; Fry, C.; Zilm, K.W.; Duchamp, J.C.; Kira, M.; Iwamoto, T.; Müller, T.; Apeloig, Y. A solid-state NMR and theoretical study of the chemical bonding in disilenes. *J. Am. Chem. Soc.* **1997**, *119*, 4972–4976. [CrossRef]
24. Obeid, N.M.; Klemmer, L.; Maus, D.; Zimmer, M.; Jeck, J.; Bejan, I.; White, A.J.P.; Huch, V.; Jung, G.; Scheschkewitz, D. (Oligo)Aromatic Species With One or Two Conjugated Si=Si Bonds: Near-IR Emission of Anthracenyl-Bridged Tetrasiladiene. *Dalton Trans.* **2017**, *46*, 8839–8848. [CrossRef] [PubMed]
25. Weidenbruch, M.; Willms, S.; Saak, W.; Henkel, G. Hexaaryltetrasilabuta-1,3-diene: A molecule with conjugated Si=Si double bonds. *Angew. Chem. Int. Ed. Engl.* **1997**, *36*, 2503–2504. [CrossRef]
26. Uchiyama, K.; Nagendran, S.; Ishida, S.; Iwamoto, T.; Kira, M. Thermal and photochemical cleavage of Si=Si double bond in tetrasila-1,3-diene. *J. Am. Chem. Soc.* **2007**, *129*, 10638–10639. [CrossRef] [PubMed]
27. Iwamoto, T.; Ishida, S. Multiple bonds with silicon: Recent advances in synthesis, structure, and functions of stable disilenes. In *Structure and Bonding: Functional Molecular Silicon Compounds II*; Scheschkewitz, D., Ed.; Springer: Cham, Switzerland, 2017; Volume 156, pp. 125–202.
28. Kosai, T.; Iwamoto, T. Stable push–pull disilene: Substantial donor–acceptor interactions through the Si=Si double bond. *J. Am. Chem. Soc.* **2017**, *139*, 18146–18149. [CrossRef] [PubMed]
29. Cowley, M.J.; Abersfelder, K.; White, A.J.; Majumdar, M.; Scheschkewitz, D. Transmetallation reactions of a lithium disilenide. *Chem. Commun.* **2012**, *48*, 6595–6597. [CrossRef] [PubMed]
30. Auer, D.; Strohmann, C.; Arbuznikov, A.V.; Kaupp, M. Understanding substituent effects on ^{29}Si chemical shifts and bonding in disilenes. A quantum chemical analysis. *Organometallics* **2003**, *22*, 2442–2449. [CrossRef]
31. Mazik, M.; Buthe, A.C.; Jones, P.G. C–H···Br, C–Br···Br, and C–Br···π interactions in the crystal structures of mesitylene- and dimesitylmethane-derived compounds bearing bromomethyl units. *Tetrahedron* **2010**, *66*, 385–389. [CrossRef]
32. Safin, D.A.; Babashkina, M.G.; Robeyns, K.; Garcia, Y. C–H···Br–C vs. C–Br···Br–C vs. C–Br···N bonding in molecular self-assembly of pyridine-containing dyes. *RSC Adv.* **2016**, *6*, 53669–53678. [CrossRef]
33. Cavallo, G.; Metrangolo, P.; Milani, R.; Pilati, T.; Priimagi, A.; Resnati, G.; Terraneo, G. The halogen bond. *Chem. Rev.* **2016**, *116*, 2478–2601. [CrossRef] [PubMed]
34. Pati, N.N.; Kumar, B.S.; Chandra, B.; Panda, P.K. Unsymmetrical bipyrrole-derived β-tetraalkylporphycenes and C–H···Br–C interaction induced 2d arrays of the 2:1 supramolecular sandwich complex of their *cis-*/*trans*-dibromo isomers. *Eur. J. Org. Chem.* **2017**, 741–745. [CrossRef]
35. Ichinohe, M.; Arai, Y.; Sekiguchi, A.; Takagi, N.; Nagase, S. A new approach to the synthesis of unsymmetrical disilenes and germasilene: Unusual ^{29}Si NMR chemical shifts and regiospecific methanol addition. *Organometallics* **2001**, *20*, 4141–4143. [CrossRef]
36. Kosai, T.; Ishida, S.; Iwamoto, T. Heteroaryldisilenes: heteroaryl groups serve as electron acceptors for Si=Si double bonds in intramolecular charge transfer transitions. *Dalton Trans.* **2017**, *46*, 11271–11281. [CrossRef] [PubMed]
37. Weitz, I.S.; Rabinovitz, M. The application of C_8K for organic synthesis: Reduction of substituted naphthalenes. *J. Chem. Soc. Perkin Trans.* **1993**, *1*, 117–120. [CrossRef]
38. Hengge, E.; Bauer, G.; Marketz, H. Darstellung und Eigenschaften einiger asymmetrisch substituierter 1,1,1-Trimethyldisilan-Verbindungen. *Z. Anorg. Allg. Chem.* **1972**, *394*, 93–100. [CrossRef]
39. Kira, M.; Hino, T.; Kubota, Y.; Matsuyama, N.; Sakurai, H. Preparation and reactions of 1,1,4,4-tetrakis(trimethylsilyl)butane-1,4-diyl dianion. *Tetrahedron Lett.* **1988**, *29*, 6939–6942. [CrossRef]

40. Sheldrick, G.M. *SADABS*; Empirical Absorption Correction Program; University of Göttingen: Göttingen, Germany, 1996.
41. Sheldrick, G.M. *SHELXL-2014/7*; Program for the Refinement of Crystal Structures; University of Göttingen: Göttingen, Germany, 2014.